CONFIGURATION DESIGN OF A ROADABLE AIRCRAFT FIXED A RING WING

M. Nakajima, Y. Nishimiya, H. Kikukawa
Kanazawa Institute of Technology
7-1 Ohgigaoka, Nonoichi, Ishikawa, 921-8501
Japan

OVERVIEW

The present author have been investigated a canard type roadable aircraft fixed a ring wing as for the future vehicle. The designed concept is introduced and aerodynamic characteristics are described in this research. The first model designed by us was improved based on CFD simulation results and estimations of control surfaces, then, the wind tunnel test was conducted for the second model. It is clarified that this roadable aircraft can meet the requirement of static directional stability and control surfaces, on the other hand, it needs a trimming device to get the wide range of the center of gravity for static longitudinal stability.

1. INTRODUCTION

As for a possible future vehicle, several types of roadable aircrafts have been studied recently[1]. We have been investigated a compact type roadable aircraft[2]-[4]. When a roadable aircraft is driven on road, its dimension has to be restricted by Road Traffic Act, which indicates that the wing span cannot be large. On the other hand, an enough wing size is needed to keep a load in flight. In order to solve this antinomy, we selected an inflatable ring wing which can be extended in flight and retracted in road. An inflatable wing should be pressurized internally to keep its ring shape. We have presented the displacement and stress of ring wing by FEA, and an effect of deformation of a ring on aerodynamics forces by CFD simulation and wind tunnel test. In this research, CFD simulation and wind tunnel test were conducted to predict the aerodynamic characteristic of a roadable aircraft designed by us. Furthermore, the position and size of control surfaces were decided based on the result of static stability estimation and the requirement of control derivative for low speed airplane.

2. DESIGNE CONCEPT OF A ROADABLE AIRCRAFT

Design specification is shown in table 1. We estimated that the gross mass of a roadable aircraft for two man crew is 800kg. The designed speed is 100knots at flight in air, and 80km/h at driving on road. Table 2 is the restriction due to Road Traffic Act in Japan. The size of a roadable aircraft on ground has to be less than these sizes. Therefore, we selected an inflatable ring wing which can be extended in flight and retracted in road.

3. FIRST ROADABLE AIRCRAFT MODEL

Figure 1 shows the first roadable aircraft model designed by us. This is a canard type aircraft. A ring wing can be retracted in road like Fig. 1(b). The airfoils of wing and canard are NACA2412 and NACA4412. The wing and the canard are fixed on body at incident of 3 degrees and 8 degrees, respectively. The length L , height H , and width W are 5.78m, 4.09m, and 5.4m in flight, respectively.

TAB 1. Design Specifications.

Item	Target	Note
Gross mass	800kg	
Engine	59.4kg	SXE-3000
Passenger	2	Side by side
Cruise speed	100knots	
Ground speed	80km/h	
Range	250km	
Takeoff runway length	300m	
Landing runway length	200m	

TAB 2. Road Traffic Act in Japan.

Item	Limit
Length	< 12.0m
Width	< 2.5m
Height	< 3.8m

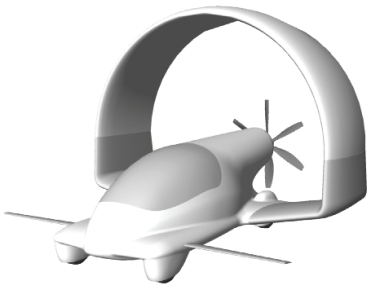

(a) in flight

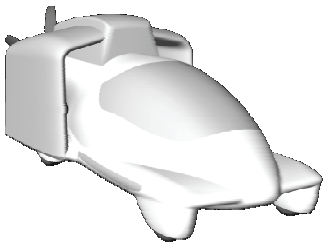

(b) on ground

FIG 1. First model roadable aircraft designed by us

3.1. CFD simulation

In order to predict the aerodynamic characteristics of the roadable aircraft, CFD simulations was performed using a commercial software, SCRYU/Tetra version 6.0, where a finite volume method and an unstructured grid system are adapted. The flow was assumed to be steady and incompressible. The $k-\varepsilon$ model with wall functions was used for the turbulence model. Figure 2 shows the computational domain. The domain consists of a rectangular box of $7L$ x $6H$ x $6W$, and the vehicle nose was located at $2L$ from the inlet. Simulations are performed for a half model using symmetry conditions in span direction. The inlet velocity was set to be 51.44m/s (100knots), and the static pressure of 0 Pa was imposed on the outlet boundary. The no-slip condition was assumed on the vehicle surface boundary, while the free slip condition was imposed on the other imaginary boundaries. A grid distribution around the vehicle is shown in Fig. 3. Four million cells were used as the entire volume mesh. In this research, stability coordinate system is used to process data.

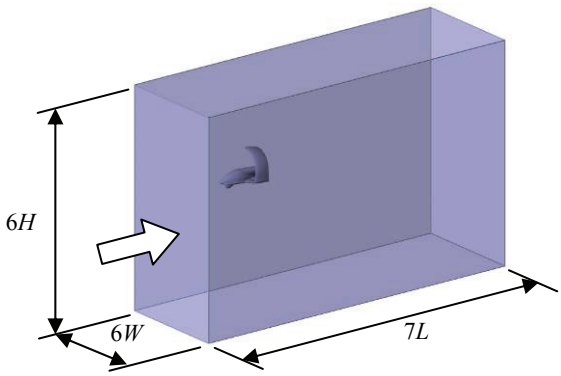

FIG 2. Computational domain

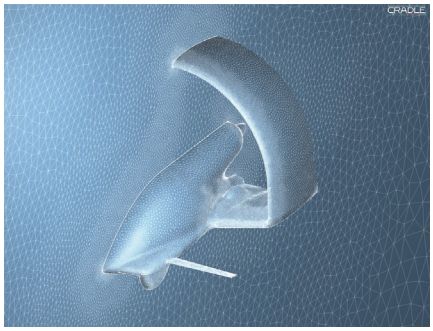

FIG 3. Surface mesh around vehicle

Figure 4 shows the lift and drag coefficients for ring wing only, ring wing plus body, and roadable aircraft with canard. These are non-dimensionalized using inlet velocity and wing area, 9.91m^2. The angle of attack of the ring wing only for free stream is subtracted 3 degrees in order to make it easy to compare with the results of roadable aircraft. In the case of the roadable aircraft with canard, it is clear that lift enough to support the 1G flight mass is produced at angle of attack 0 degree. At angle of attack 0 degree, the body produces about 35 % of the total lift. The stalling angle of roadable aircraft comes around 8 degrees, which is smaller angle of attack than the ring wing only. This stall starts form body. The body shape should be re-designed to get large stall angle. Figure 5 is the pitching moment coefficient about the body nose. These are non-dimensionalized using wing mean chord 2.102m. From these results, the range of center of gravity was set less than 50% of the vehicle length in order to meet the requirement that the static longitudinal stability is less than -0.01.

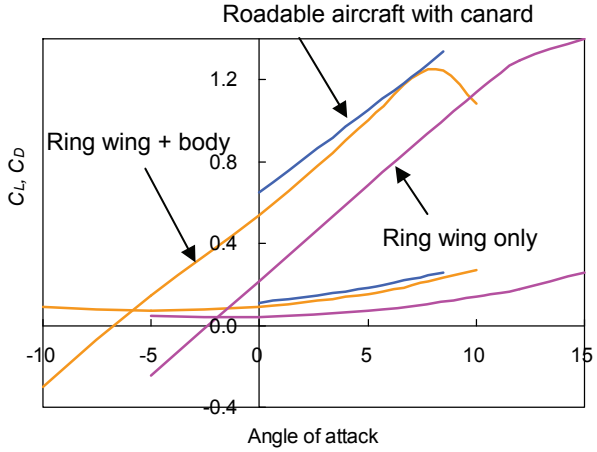

FIG 4. Lift and drag coefficients by CFD simulation

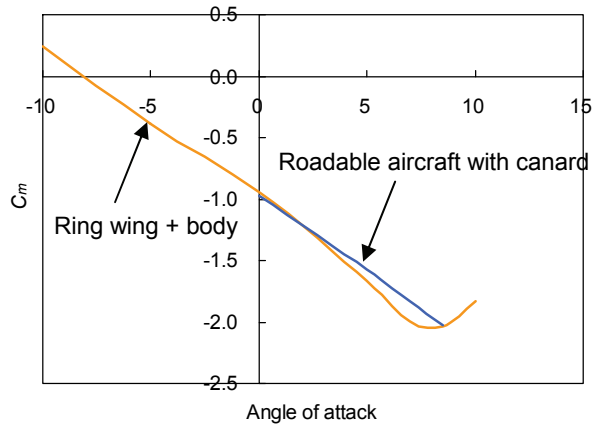

FIG 5. Pitching moment coefficient by CFD simulation

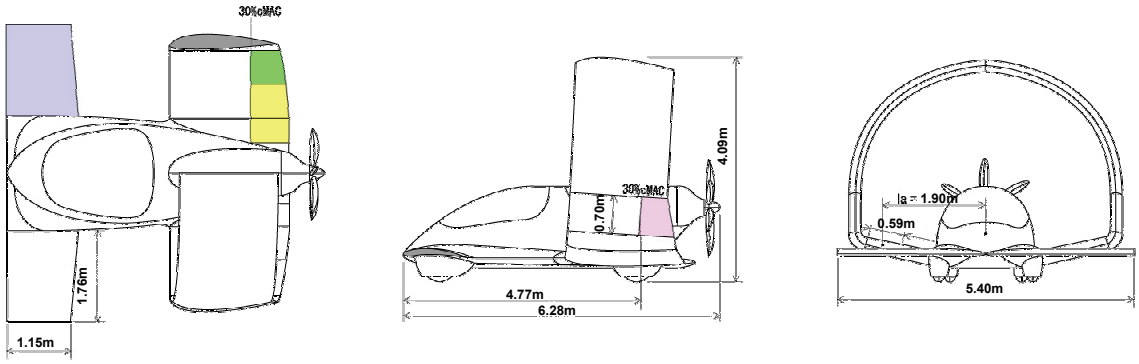

FIG 6. Positions of control surfaces

TAB 3. Design requirement of control surface derivative.

Item	Maximum control angle	Design requirement of control derivative
Elevator	±25°	$\frac{dC_m}{d\delta_c} = 0.017 \quad - \quad 0.022$
Rudder	±30°	$\frac{dC_n}{d\delta_r} = 0.001 \quad - \quad 0.0012$
Aileron	+25°	$\frac{dC_m}{d\delta_a} = 0.0034 \quad - \quad 0.0043$
	-15°	

3.2. Design of control surfaces

Low speed airplane has control derivative as shown on table 3. We designed control surfaces to meet these requirements, and studied the allowable range of center of gravity. The control derivative were estimated using these equations,

(1) $$\frac{dC_m}{d\delta_c} = \frac{dC_{Lc}}{d\delta_c} \cdot \frac{l_c S_c}{cS}$$

(2) $$\left(\frac{dC_{Lc}}{d\delta_c}\right)_{3D} = \left(\frac{dC_{Lc}}{d\delta_c}\right)_{2D} \cdot \frac{k}{1 + 2k/AR}$$

(3) $$\left(\frac{dC_{Lc}}{d\delta_c}\right)_{2D} = 2\left\{\sqrt{1-(1-2r)^2} + \cos^{-1}(1-2r)\right\}$$

These equations are shown using the parameters for the canard case. c, S, l_c, S_c, AR, k, r are wing chord, wing area, moment arm to the center of gravity, canard area, canard aspect ratio, airplane efficiency and ratio of canard, respectively.

TAB 4. Specifications of control surfaces.

Wing	
Wing area	9.91m^2
Wing chord	0.210m
Canard	
Canard span	3.510m
Canardvator chord : c_{f_c}	1.241m
Canard chord : c_c	1.241m
Ratio of canard : c_{f_c} / c_c	1.000
Airplane efficiency	0.800
Nose to 25%canard chord	0.454m
Canard area	4.356 m^2
Canard aspect ratio	2.828
Rudder	
Rudder span	0.700m
Rudder chord	0.560m
Vertical tail chord	1.880m
Ratio of rudder	0.298
Airplane efficiency	0.800
Nose to 25%Ch	3.930m
Vertical tail area	1.316 m^2
Vertical tail aspect ratio	1.804
Aileron	
Aileron span	0.590m
Aileron chord	0.630m
Horizontal tail chord	2.110m
Ratio of aileron	0.299
Airplane efficiency	0.800
Body center to 50%aileron	1.910m
Aileron area	1.245 m^2
Horizontal tail ratio	2.237

When the canard size and the vehicle length of the first model in Fig.1 were used to estimate the canard control power, the values didn't meet the requirement. Therefore, the vehicle length was stretched 0.5m, and the canard area was enlarged. The position and specifications of control surfaces for the stretched model are shown in Fig. 6 and on table 3, respectively. The vehicle length and the canard area are 1.9m^2 and 6.4m. The range of center of gravity which can be satisfied the requirements are shown on table 4. It is clear that all requirements can be satisfied in the range of center of gravity, 30% to 50%.

TAB 5. Range of center of gravity.

Control surface	Control Derivative	Range of the center of gravity met design requirement (20% to 50%)
Roadable aircraft	C_{m_α}	< 50%
Canard	$C_{m_{\delta c}}$	> 30%
Rudder	$C_{n_{\delta r}}$	20% < 50%
Aileron	$C_{l_{\delta a}}$	20% < 50%

4. RE-DESIGNED ROADABLE AIRCRAFT MODEL (THE SECOND MODEL)

Figure 7 is the second model. Furthermore, body shape was refined to improve stall characteristic. In order to investigate the aerodynamic characteristics of this model, wind tunnel test was conducted.

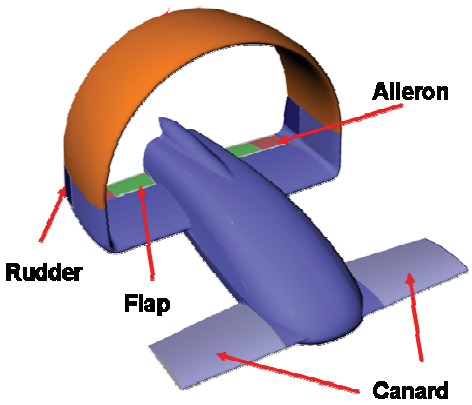

FIG 7. Re-designed model(the second model)

FIG 8. Wind tunnel model

FIG 9. Wind tunnel test section

5. WIND TUNNEL TEST

The second model was tested using Gottingen wind tunnel which has 2m x 2m test section, its maximum velocity is 80m/s. Figure 8 is the wind tunnel model. The model is supported by a sting installed a six-component internal balance as shown in Fig. 9. Free stream velocity was set 40m/s. Smoke and tuft flow visualization was also performed. Aerodynamic coefficients are shown in Fig. 10 and 11. These values are non-dimensionalized using free stream velocity, wing area 0.0991m^2, mean wing chord 0.2102m, and wing span 0.472m. The center of gravity was set at the position of 40% vehicle length from nose.

Figure 10 shows lift, drag and pitching moment coefficients. The results of the roadable aircraft without canard are also shown. Lift enough to support the 1G flight mass is produced at angle of attack 0 degree. Canard produces about 15 % of total lift. Stall angle is about 15 degrees, which is improved than the first model. It is confirmed from flow visualization that stall starts from canard, not body. It is clear that the longitudinal static stability of roadable aircraft is not kept because the effectiveness of canard for pitching is strong, therefore, the position of the center of gravity and canard area have

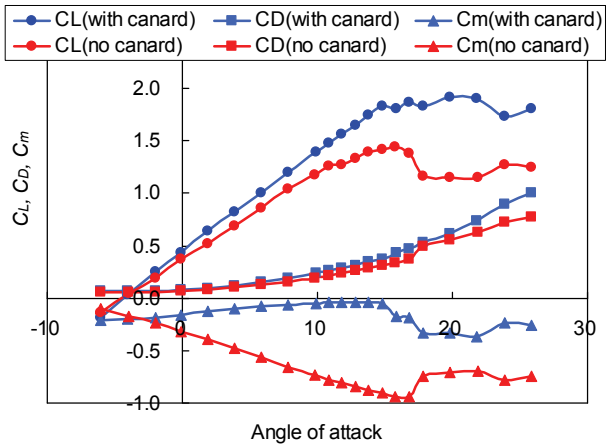

FIG 10. Lift, drag and pitching moment coefficients for re-designed model

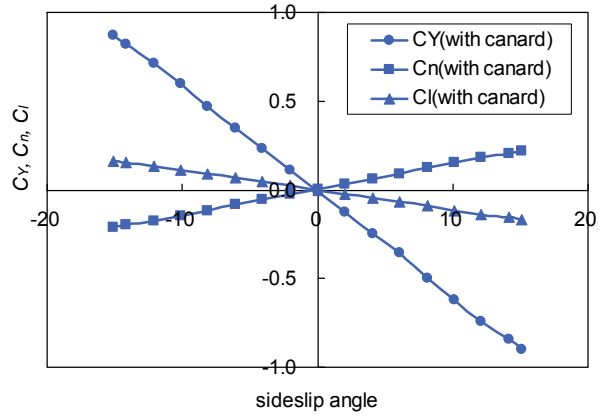

FIG 11. Side force, yawing and rolling moment coefficients for re-designed model

to be changed. Figure 11 shows side force, yawing moment, and rolling moment coefficients. It is found that directional static stability is kept as the derivative is positive. Furthermore, negative rolling moment is produced when the sideslip angle is positive. This means that aileron have to be controlled when sideslip is happened. The aileron angle required when the rudder is controlled at 30 degrees is estimated using these equations,

(4) $C_{n_{\delta r}} \cdot \delta_r + C_{n_{\delta a}} \cdot \delta_a + C_{n_\beta} \cdot \beta = 0$

(5) $C_{l_\beta} \cdot \beta + C_{l_{\delta r}} \cdot \delta_r + C_{l_{\delta a}} \cdot \delta_a > 0$

where, β, δ_a, δ_r are sideslip angle, aileron angle, and rudder angle. These parameters are shown on table 4. Required canard angle is estimated to 4.19 degrees. It is clear that the roadable aircraft can control sideslip.

TAB 6. Evaluation of sideslip.

Item	Value
Dihedral effect : C_{l_β}	-0.0107
Rolling moment due to rudder derivative : $C_{l_{\delta r}}$	0.0013
Roll control power : $C_{l_{\delta a}}$	0.0018
Static directional stability : C_{n_β}	0.0148
Rudder control power : $C_{n_{\delta r}}$	-0.0021
Rudder angle: δ_r	30.0
Sideslip angle: β	4.20
Canard angle: δ_a	4.19

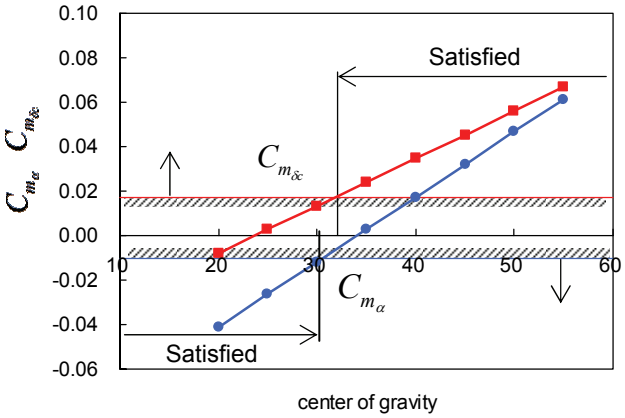

FIG 12. Static longitudinal stability and canard control power(original canard area)

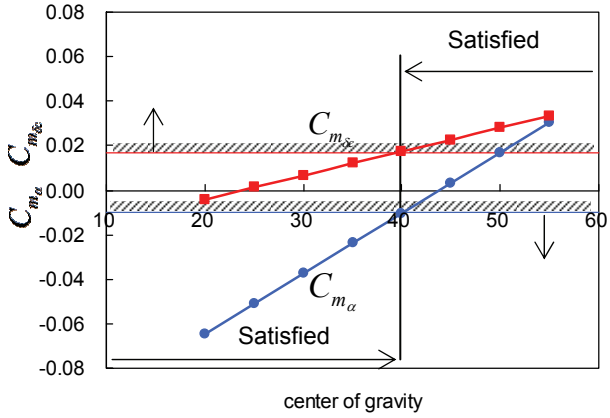

FIG 13. Static longitudinal stability and canard control power(half canard area)

In order to check the effect of control surfaces, the control derivatives were calculated for the range of the center of gravity 20% to 55%. Figure 11 shows the static longitudinal stability and the canard control power. The rudder control power is 0.0014 to 0.0042, which has enough power. It is obvious that the second model does not have the range of center of gravity in which the requirements of both the static longitudinal stability and the canard power are satisfied. In order to find a condition which can be satisfied the requirement, the canard area was changed assuming that the canard control power to proportionate to area. Figure 12 shows the case of the half canard area. The requirement is satisfied at the only 40% center of the gravity. We will solve this difficulty by installing stability tab on the canard surface to improve power. The aileron control power is 0.0018, which does not meet the requirement, more than 0.0034. We think that this can be solved controlling a rudder together.

6. CONCLUSION

The aerodynamic characteristics of the canard type roadable aircraft was tested using a wind tunnel. Obtained conclusions the follows:

(1) The roadable aircraft can produce lift enough to support the 1G flight mass, 800kg at the angle of attack 0 degree.

(2) The maximum lift coefficient is about 1.8. The stall angle is 15 degrees, and the stall starts from canard first.

(3) When the vehicle is in sideslip, large rolling moment also is produced with yawing. Therefore, aileron has to be controlled together.

(4) Canard control power has to be improved by installing stability tab to get the wide range of the center of gravity in longitudinal stability.

7. REFERENCES

[1] R. N. McGrath, “Economic Viability of NASA’s Next-Generation Aviation Paradigm, A Summary of Research Fondings“, SAE Paper 2002-01-2924, (2002).

[2] M. Nakajima, T. Fukasawa, H. Kikukawa and T. Fukasawa, “Design of a Roadable Aircraft of Fixed Wing and the investigation ogf the aerodynamics characteristics“, SAE Paper 2004-01-3124, (2004).

[3] M. Nakajima, A. Yanagisawa, H. Kikukawa and T. Fukasawa, “Investigations on Inflatable Ring Wing of a Compact Type Roadable Aircraft“, SAE Paper 2005-01-3422, (2005).

[4] M. Nakajima, Y. Nishimiya and H. Kikukawa, “Aerostructual Study on Inflatable Wing of a Roadable Aircraft“, 15th AIAA/ASME/AHS Adaptive Structure Confarence, Hawaii, AIAA Paper 2007-2330, CD-ROM Number 7.